International Journal of Pharmaceutics 664 (2024) 124595

Contents lists available at ScienceDirect

International Journal of Pharmaceutics

journal homepage: www.elsevier.com/locate/ijpharm

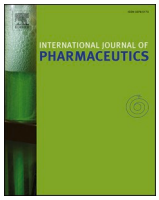

Physicochemical characterization of the metamorphosis of film-forming formulations of betamethasone-17-valerate

Panagiota Zarmpi [a], Andrea Pensado [a], Sergey N. Gordeev [b], K.A. Jane White [c], Annette L. Bunge [d], Richard H. Guy [a], M. Begoña Delgado-Charro [a,*]

[a] University of Bath, Department of Life Sciences, Claverton Down, Bath BA2 7AY, UK
[b] University of Bath, Department of Physics, Claverton Down, Bath BA2 7AY, UK
[c] University of Bath, Department of Mathematical Sciences, Claverton Down, Bath BA2 7AY, UK
[d] Colorado School of Mines, Department of Chemical & Biological Engineering, Golden, CO 80401, USA

ARTICLE INFO

Keywords:
Topical product metamorphosis
Film-forming systems
Spray formulations
Confocal Raman microspectroscopy
In vitro release testing

ABSTRACT

Following topical application of a dermatological product, the loss (by evaporation and/or absorption through the skin) of volatile excipients will alter the composition of the formulation remaining on the tissue. This so-called metamorphosis impacts the concentration of the drug in the residual vehicle, (potentially) its physical form therein and, as a result, its uptake into and subsequent permeation through the skin. This research aimed to characterise – using primarily confocal Raman microspectroscopy – the metamorphosis of film-forming formulations of betamethasone-17-valerate (at different loadings) comprised of hydroxypropyl cellulose (film-forming agent), triethyl citrate (plasticizer) and ethanol (solvent). Dissolved and crystalline drug in the films were identified separately by their different characteristic Raman frequencies (1666 cm^{-1} and 1659 cm^{-1}, respectively). These Raman measurements, as well as optical imaging, confirmed corticosteroid crystallisation in the residual films left after ethanol evaporation when drug concentration exceeded the saturation limit. In vitro release tests of either sprayed or pipette-deposited films into either aqueous or ethanolic receptor solutions revealed drug release kinetics dominated by the residual film post-metamorphosis. In particular, the rate and extent of drug release depends on the concentration of dissolved drug in the residual film, which is limited by drug saturation unless supersaturation occurs. For the simple films examined here, supersaturation was not detected and the solubility limit of drug in the films was sufficient to sustain drug release at a constant flux from the saturated films through a thin silicone elastomer membrane into an aqueous receptor solution for 30 h. Flux values were ~ 1 μg $cm^{-2}h^{-1}$ from saturated residual films independent of the amount of crystallized drug present. Flux from subsaturated films was reduced by an amount that was consistent with the lower degree of saturation.

1. Introduction

Drug administration by topical or transdermal routes is attractive but challenging due to the barrier properties of the stratum corneum (SC). Active ingredients must be lipophilic enough to partition into the SC, but not so much that partitioning into the more aqueous deeper layers of the skin tissue becomes limiting. Often, topically applied molecules suffer from limited solubility in common dermatological vehicles, which makes the incorporation of volatile excipients (co-solvents) necessary to facilitate drug permeation into the tissue. However, when a product containing one or more volatile ingredient is applied to skin its composition (i.e., the relative levels of drug and excipients) and the physical form of the active may change significantly. This transformation, referred to as *metamorphosis* (Surber and Davis, 2002), can have a complex impact on the kinetics and extent of drug release to and permeation through the skin.

As illustrated in Fig. 1, upon application of a formulation, volatile ingredients may rapidly partition into the SC and facilitate the transfer of drug (Chang et al., 2013). Simultaneously, volatile excipients evaporate causing the drug concentration to increase as a 'new' residual phase forms on the skin surface, thereby increasing the driving force for the active to partition into and diffuse across the SC (Shah et al., 1993).

* Corresponding author.
E-mail address: B.Delgado-Charro@bath.ac.uk (M. Begoña Delgado-Charro).

https://doi.org/10.1016/j.ijpharm.2024.124595
Received 29 May 2024; Received in revised form 13 August 2024; Accepted 15 August 2024
Available online 16 August 2024

As the drug concentration reaches its saturation limit in the residual phase, the theoretical maximum flux across the skin will be achieved although, at this point, it is also conceivable that a transient, supersaturated state may occur (Leichtnam et al., 2006a,b; Moser et al., 2001), which can increase transport beyond the limiting point achieved with saturation (Davis and Hadgraft, 1991). Inevitably, of course, the thermodynamic instability of a supersaturated solution ensures that precipitation/crystallisation of the drug occurs and, depending on the equilibrium solubility of the compound in the residual film, this will then determine the subsequent rate and extent of skin penetration (Frederiksen et al., 2016). Incorporating non-volatile ingredients that delay evaporation of volatiles and/or extend the duration of supersaturation have enhanced the skin delivery of corticosteroids (Reid et al., 2013).

This complex metamorphosis behaviour is observed in both simple vehicles and conventional formulations, such as creams and gels, and has been implicated in the poor performance of many topical drug products (Lippold and Schneemann, 1984; Oakley et al., 2021; Surber and Knie, 2018). The increased appreciation of the significance of a formulation's physical transformation upon application to the skin leads to two important conclusions: first, that there are innovator drug products used in dermatology that are therapeutically effective but pharmaceutically inefficient in terms of drug delivery (i.e., the percentage of the drug 'dose' applied that is absorbed to the site of action is measured in single digits or less); and, second, that an important barrier to the approval of generic products has been created. This is because the demonstration of topical equivalence requires matching a (not unusually) mediocre level of performance while ensuring that qualitative (Q1) and quantitative (Q2) sameness is achieved, and providing evidence that the critical physicochemical and structural characteristics (Q3) of the generic formulation mirror those of the reference product (FDA, 2022). The latter requirement, put another way, implies that the metamorphosis of a generic product to the residual phase post-application must be demonstrated to proceed in an identical manner as that of the innovator formulation.

The importance of understanding drug product metamorphosis with respect to the development of high-performance topical formulations is clear. Optimal design of not only the packaged product, but also of the residual film, and control of the transformation of one to the other, are essential elements involved in metamorphosis, especially when multi-component vehicles are involved, and pose significant challenges for both experimental characterization and predictive dermatopharmacokinetic modelling (Bunge, 1998; Parks et al., 1997).

To begin to 'unpick' the problem, a useful starting point for investigation is the relatively simple film-forming system (FFS). In a straightforward embodiment, these formulations typically comprise a polymeric film-forming agent, a plasticizer, and the chosen drug dissolved or dispersed in a volatile solvent. Upon application to the skin, typically by spraying, a flexible film adaptable to skin movement forms *in situ* as the solvent evaporates (Frederiksen et al., 2016). The superior performance of such formulations compared to conventional products (e.g., creams) has been demonstrated (Reid et al., 2013). The physicochemical status of the drug in the film (dissolved at less than its saturation limit, precipitated and dissolved at its saturation limit, or dissolved at supersaturation) is potentially manipulable by the FFS composition, the drug loading, and the kinetics of metamorphosis (Edwards et al., 2017; Frederiksen et al., 2015). The goal of the research described here was to characterize FFSs comprising hydroxypropyl cellulose, triethyl citrate, and various loadings of betamethasone-17-valerate in ethanol. The impact of FFS metamorphosis has been deduced – as functions of the film preparation method and aging – using, primarily, confocal Raman microspectroscopy and *in vitro* release testing, supplemented with profilometry and optical and atomic force microscopy measurements.

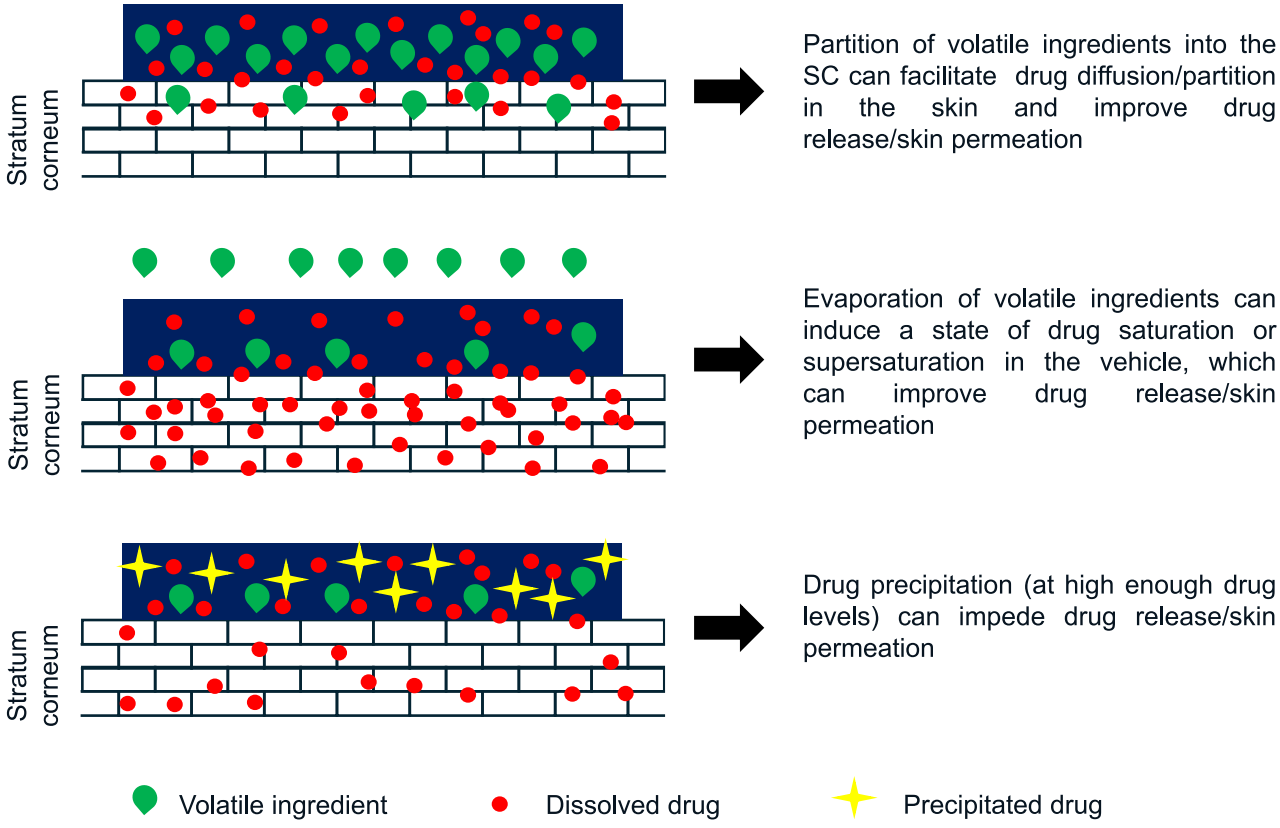

Fig. 1. Likely events occurring upon the loss (by evaporation and/or SC uptake) of the volatile ingredient(s) and the resulting influence on topical drug release to and permeation through the skin.

2. Materials and methods

2.1. Materials

Betamethasone-17-valerate (BMV-17; European Pharmacopeia Reference Standard) was supplied by Fagron UK, Ltd. (Newcastle upon Tyne), betamethasone-21-valerate (BMV-21; European Pharmacopeia Reference Standard) betamethasone (BM; minimum 98 %) and polyethylene glycol hexadecyl ether (Brij 58®) were from Sigma Aldrich (Gillingham, UK), hydroxypropyl cellulose (HPC; Klucel-LF) was obtained from Ashland, Inc. (Wilmington, DE), and triethyl citrate (TEC) was purchased from Thermo Fischer Scientific (Loughborough, UK). Sodium chloride, potassium chloride sodium phosphate dibasic anhydrous, potassium phosphate monobasic were from Fischer Scientific (Loughborough, UK). High-performance liquid chromatography (HPLC) grade acetonitrile (ACN) and absolute ethanol (EtOH) were obtained from VWR (Lutterworth, UK). Water was ultra-pure (Milli-Q) laboratory grade.

2.2. Preparation of BMV-17 loaded film-forming systems (FFSs)

The drug-free FFS was prepared by mixing HPC (5 % w/w) and TEC (1 % w/w) in EtOH and stirring for 24 h to ensure complete dissolution. The FFS formulations were then prepared by adding BMV-17 to achieve BMV-17 loadings of 0.05, 0.10, 0.20, 0.50, 1, 3, 5 and 10 % (mass ratio of BMV-17 to drug-free FFS) and equilibrating for 24 h at 32 °C. The actual polymer and drug contents in the FFS formulations and in the residual films post EtOH evaporation, and the drug-to-polymer ratio in the latter, are listed in Table 1 and, in more detail, in **Table S1**.

2.3. Selection of spraying parameters

Sprayed FFS films were prepared using a mini air brush compressor (AB900.v3, Sealey Power Products, Bury St Edmunds, UK) equipped with a spray gun (AB9321), oriented perpendicular to the chosen substrate to permit spraying at a limited range (**Figure S1**). In initial studies, films without BMV-17 were sprayed onto Parafilm® (Bemis Company, Inc., Neenah, WI, USA) and glass microscope slides (7.5 cm x 2.5 cm x 1 mm; Fischer Scientific, Loughborough, UK). The purpose of these experiments, respectively, was to assess (i) film flexibility, and (ii) film condition (completeness and homogeneity), dryness after 5 min, and stickiness (Frederiksen et al., 2015). A spacer, with an opening of 5.5 cm x 1.5 cm area, was made by hand (using a scalpel) with one-sided adhesive tape (synthetic acrylic adhesive on a polypropylene backing (3 M Scotch tape, ScotchBrand, UK) and was placed in the middle of each microscope slide. Approximately 3 g of the FFS were sprayed onto the glass slide (or Parafilm) using spray nozzles with 0.2 mm, 0.3 mm, and 0.5 mm diameter openings at distances of approximately 0 cm, 5 cm, and 10 cm from the glass surface. The FFS was sprayed by moving the spray gun horizontally across the 5.5 cm x 1.5 cm area delimited by one spacer; some of the FFS was deposited outside this area. It was found that spraying with a 0.3-mm nozzle from 10 cm produced films that were dry after 5 min and homogeneously covered the sample area (see **Table S2**). Sprayed films in all subsequent studies used this procedure.

2.4. Physical form and distribution of BMV-17 in the sprayed films

In this component of the work, approximately 3 g of FFSs containing 1, 3, 5 and 10 % (w/w) BMV-17 were sprayed onto glass microscope slides. The target area this time was 2 x 2 cm^2 which was delimited with two spacers (prepared as before), with one placed directly over the second. Again, it was impossible to avoid deposition of some of the FFS outside the delimited area. The spacers were then removed, and the treated glass slides were stored at 32 °C and 35 % relative humidity (RH) for 24 h to allow for complete solvent evaporation.

To assess the extent that drug crystallisation had occurred within the dried films, imaging with optical microscopy (80i Nikon Eclipse, Nikon Corporation, Tokyo, Japan) was performed; the physical form of BMV-17 (dissolved or crystalline) and its distribution within the films were assessed using confocal Raman microscopy (inVia, Renishaw, Wotton-Under-Edge, UK). Raman maps of the films were acquired over areas of 80 μm x 70 μm. The excitation source was a laser operating at 532 nm using 10 % of its maximum power to prevent burning of the sample. A 20x working distance objective lens was used. Samples were exposed for 10 s to the laser beam and a single accumulation was obtained from an area of approximately 1 μm x 1 μm (which corresponded to the area of each pixel in the chemical map). Characteristic Raman peaks at 1458 cm^{-1} (CH_2 bending) for HPC, 1666 cm^{-1} (C=O stretching) for BMV-17, and 1736 cm^{-1} (C=O stretching) for TEC were identified, as previously reported (Garvie-Cook et al., 2015a).

The physical form of BMV-17 was determined from the position of its C=O stretching peak; maximum signal intensities at 1666 cm^{-1} and 1659 cm^{-1} correspond to dissolved and crystalline BMV-17, respectively (Garvie-Cook et al., 2015b). In cases where dissolved and crystalline BMV-17 signals overlapped, deconvolution was undertaken using curve-fitting (WiRE software v1.2, Renishaw plc). Peak parameters (centre, width, % Gaussian) of the underlying dissolved and crystalline signals were defined and fit to the overlapping BMV-17 signal for deconvolution. The distribution of the dissolved BMV-17 across the surface of films was assessed from the intensity of the 1666 cm^{-1} peak. Drug intensities were normalised according to the intensity of HPC in each pixel to facilitate comparisons between different experiments and instrument settings and to 'correct' for other factors that introduce intensity variability into the spectra (Zarmpi et al., 2023).

2.5. Estimation of drug solubility in the residual phase using confocal Raman spectroscopy

Additional residual films were prepared from FFSs with lower BMV-17 content (0.05 %, 0.10 %, 0.20 % and 0.50 % w/w) by spraying 1.5 g of each formulation onto a 2 x 2 cm^2 area delimited by a laboratory-made spacer (see above). The dissolved BMV-17 in these films

Table 1
Drug loadings (mass ratio of BMV-17 to FFS non-drug constituents), polymer and drug mass fractions in the FFS formulations and the post-EtOH evaporation films, and the drug-to-polymer mass ratio. Film values are calculated assuming that no EtOH is present in the residual phase after 24 h.

BMV-17 loading in the FFS (%)	HPC (%)		BMV-17 (%)		BMV-17:HPC ratio
	FFS	Film	FFS	Film	
0	5.00	83.33	–	–	–
0.05	5.00	82.64	0.05	0.83	0.01
0.1	5.00	81.97	0.10	1.64	0.02
0.2	4.99	80.65	0.20	3.23	0.04
0.5	4.98	76.92	0.50	7.69	0.10
1	4.95	71.43	0.99	14.29	0.20
3	4.85	55.56	2.91	33.33	0.60
5	4.76	45.45	4.76	45.45	1.00
10	4.55	31.25	9.09	62.50	2.00

(detected at 1666 cm^{-1}) was assessed over 10 μm x 20 μm areas using the 532 nm laser operating at its maximum laser power with a 10 s exposure time; as crystallized drug was not present, the higher laser power was used to increase the Raman signal intensity (again, without sample burning). A 50x working distance objective lens was used. The intensity of the dissolved BMV-17 peak was recorded at 1 μm intervals on three randomly selected lines (9 μm in length) along the x-axis of each map. BMV-17 intensities were normalised by the HPC intensity in each pixel and the mean and standard deviation of the 30 acquired data were calculated as functions of the drug-to-polymer ratio in the residual films and the BMV-17 loading in the FFS. For films from FFSs containing the higher drug loadings (3 % and above), in which BMV-17 crystallisation was observed, the deconvoluted peaks of only the dissolved active were used in the data analysis described below.

2.6. Profilometry and 3D topography of sprayed films

The thicknesses of the residual films prepared by spraying as described previously from FFSs containing 1, 3, 5 and 10 % BMV-17 loadings were determined with a surface profiler (Veeco 6 M Dektak Surface Profiler, Veeco instruments, Plainview, NY, US). Samples of residual films were positioned on the profiler stage and a diamond stylus tip (12 μm radius) was slowly moved down towards the surface. The film was then moved against the stylus tip, to which a vertical force of 9.8 x 10^{-6}N was applied, and changes in the height of the profile along the x-axis (3000 μm in length) were monitored. For reference purposes, measurements started outside the film on the smooth, clean surface of the glass slide. Subsequently, profiles were recorded along four lines for every film, and three films from each FFS composition were examined separately.

The 3D micro-topography of the residual films from FFSs containing 1, 3, 5 and 10 % w/w BMV-17 was assessed using atomic force microscopy (atomic force scanning probe microscope with a Nanoscope IIIA controller and running Nanoscope software (version 7.341, Veeco Instruments, Plainview, NY, US). FFSs were sprayed as before onto glass microscope slides but, in this case, a different arrangement of the substrate was used to permit AFM data to be obtained from both the film directly below the spray nozzle (the 'central' region) and from an area at the 'border' of the sprayed area. This was achieved by positioning two 1 cm x 1 cm pieces of a microscope slide side-by-side on a standard glass microscope slide; one of the pieces was directly below the nozzle, the other clearly off to one side. AFM imaging under contact mode was then undertaken 24 h post-spraying once complete solvent evaporation had occurred (32 °C and 35 % RH, as before). Attachment to the sample holder used double-sided adhesive tapes. The AFM probes employed (Veeco NP20) had spring constants ranging from 0.12 to 0.38 N m^{-1}.

2.7. Ester group migration of BMV-17

The ester group migration of BMV-17 to BMV-21 and its subsequent hydrolysis to BM was evaluated in the FFSs, the residual films, and the different receptor solutions used in the *in vitro* release tests (IVRTs) described below. FFSs with 1, 3, 5 and 10 % w/w BMV-17 loadings were prepared in glass beakers, which were tightly capped, covered with aluminum foil and stored at 32 °C. After 24, 48, 72 and 96 h, 0.3 g samples were withdrawn, filtered (4-mm diameter, 0.45-μm pore size regenerated cellulose filters; SMI-LabHut Ltd, Maisemore, UK), diluted with ACN/water 60/40 % v/v, and analysed by HPLC-UV. Migration was measured in residual films prepared by depositing (from a pipette) 0.3 g of the FFS containing 10 % w/w BMV-17 onto a plastic (polypropylene) substrate. Films were then stored at 32 °C and 35 % RH. After 0.5, 1, 2, 4, 6, 8, 24 and 30 h, the films were extracted into 20 mL of ACN/water 60/40 % v/v by shaking overnight. Extract samples (1 mL) were filtered as above, diluted as necessary, and analysed by HPLC-UV. Migration was also measured in the receptor solutions used in the IVRT experiments, both aqueous (pH 7.4 phosphate buffer saline with 0.5 % w/w Brij 58®) and organic-based (EtOH/water 60/40 % v/v) that contained either 10 or 100 μg mL^{-1} BMV-17. The receptor solution standards were prepared in glass beakers, which were tightly capped, covered with aluminum foil, and stored at 32 °C. After 0.5, 1, 2, 4, 6, 8, 24 and 30 h, 0.5-mL samples were withdrawn, filtered as above, and analysed by HPLC-UV. All migration experiments were performed in triplicate. Periodic analyses of BMV-17 standards prepared in ACN/water 60/40 % v/v showed that no ester group migration occurred upon dilution.

2.8. In vitro release tests (IVRT)

2.8.1. Aqueous-based receptor solution

Residual films from FFSs containing 1, 3, 5 and 10 % BMV-17 loadings were sprayed with the mini air brush compressor (0.3 mm spray nozzle at 10 cm from the substrate surface) onto nonporous silicone elastomer membranes (75 μm thickness; Dow Corning 7–4107, Auburn, MI, US) that had been soaked in the phosphate pH 7.4 buffer receptor solution containing 0.5 % w/w Brij 58® for 0.5 h. Approximately 1 g of each formulation was sprayed onto 2 cm x 2 cm of the membrane, the area of which was larger than that (2.0 cm^2) of the vertical Franz diffusion cells (PermeGear, Inc., Bethlehem, PA, US) used in the IVRT experiments. Five minutes after spraying, the residual film-silicone membrane composite was mounted in the diffusion cell: the residual film faced the donor compartment and the silicone membrane made direct contact with the receptor solution in the lower chamber. The receptor volume was 7.4 mL ensuring sink conditions for the drug, which was released from the residual film and then diffused through the silicone membrane. After 0.5, 1, 2, 4, 6, 8, 24 and 30 h, 1-mL samples were withdrawn from the receptor compartment, replaced with fresh solution, filtered as above, and analysed by HPLC-UV. Throughout the experiment, the diffusion cells were maintained at 32 °C and 35 % RH in an oven, except for brief excursions when the receptor solution was sampled and replaced. At the end of the experiment, the membrane was removed from the Franz cell, and that part which was exposed to the receptor solution (i.e., a circular portion of 2.0 cm^2) was carefully excised with a scalpel. This membrane portion was then extracted into 5 mL of ACN/water 60/40 % v/v with shaking overnight, after which it was filtered as above, diluted as necessary, and analysed by HPLC-UV to determine the remaining drug amount in the membrane and the residual film. The initial mass of BMV-17 in the residual film, and in contact with the diffusion area of the Franz cell, was calculated by mass balance, i.e., drug in the membrane (which includes the residual film) and the accumulated receptor solution. Mean extraction efficiencies were > 94 % for all films considered. The influence of film aging on drug release was evaluated in a series of identical IVRT experiments with films created from FFSs containing 5 and 10 % BMV-17 loadings. In these experiments, films were stored at 32 °C and 35 % RH for 2 h and 4 h before mounting in the diffusion cells. All experiments were performed in triplicate.

2.8.2. Organic-based receptor phase

IVRT experiments were also conducted using an organic-based receptor solution of EtOH/water 60/40 % v/v (which provided sink conditions). In this case, the FFSs were either sprayed (as above) or pipetted onto silicone membranes that had been soaked in the receptor solution for 30 min. The pipetted FFSs were delivered to and carefully spread with the pipette tip on membranes mounted in the Franz cells. The volume of FFS pipetted onto the membrane was chosen to provide a BMV-17 'dose' that was similar to that of the sprayed films from the same FFS. All experiments were performed in triplicate. Once again, the initial mass of BMV-17 was calculated by mass balance.

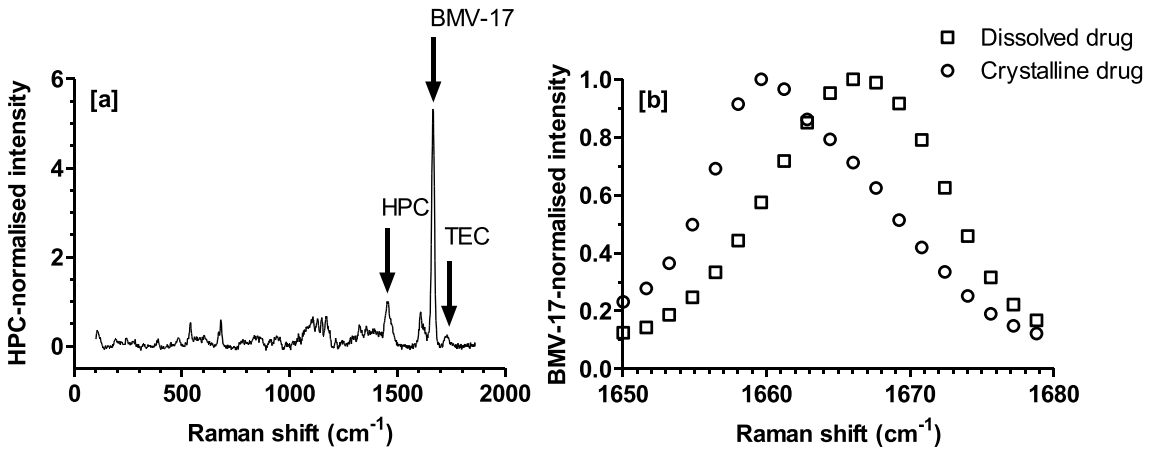

Fig. 2. (a) Representative Raman spectrum of one pixel of the maps normalised according to the HPC intensity, and (b) Raman spectra of dissolved (squares) and crystalline (circles) BMV-17 normalised according to the maximum intensity of each peak.

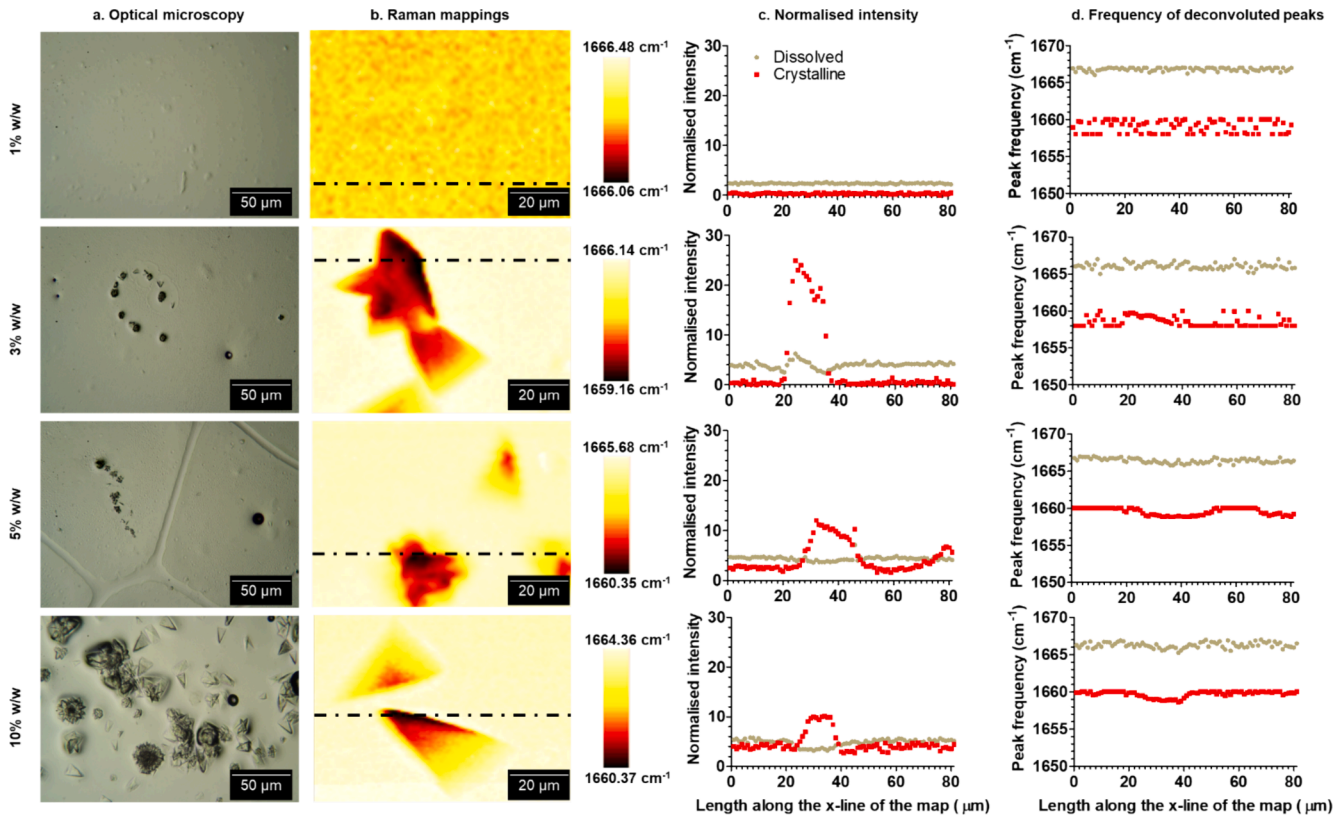

Fig. 3. Physical form and distribution of BMV-17 in residual films prepared from FFSs with 1, 3, 5 and 10 % drug loadings. (a) Optical microscopic images. (b) Raman maps of the BMV-17 peak signal and deduced physical form (dissolved drug: 1666 cm^{-1}; crystalline drug: 1659 cm^{-1}; between 1659 cm^{-1} and 1666 cm^{-1}: overlapping crystalline and dissolved drug); colour maps distinguish between different forms of the drug present (see text). (c) Deconvoluted HPC-normalised BMV-17 signal intensities along the dot-dashed lines in panel (b). (d) Deconvoluted peak frequencies of dissolved (lighter colours in panel (b)) and crystalline BMV-17 (darker colours) along the same dot-dashed lines in panel (b).

2.9. Chromatographic conditions

Drug quantification was determined by HPLC-UV (Shimadzu LC-2010, Milton Keynes, UK) using a modified version of a previously published protocol (Bundgaard and Hansen, 1981). The method consisted of 50 µL sample injections onto a reversed-phase C18 column (HiQ sil C18HS C18 column 250 mm × 4.6 mm, 5 µm, Kromatek, Dunmow, UK) at 25 °C with an ACN/water (60/40 v/v) mobile phase, a flow rate of 1 mL/min, and UV detection at 238 nm. The retention times were 11.6 min, 15.9 min and 4.9 min for BMV-17, BMV-21 and BM, respectively. Quantification of the three compounds was based on calibration curves of peak area versus concentration in standards prepared from stock solutions in ACN (1 mg/mL). The limits of detection (LoD) and quantification (LoQ) were very close for all three compounds with values of 0.006–0.008 and 0.018–0.024 µg/mL, respectively.

2.10. EtOH evaporation from FFSs

Ethanol evaporation after deposition of the FFSs was measured by weight loss using an analytical balance (BP 210D, Sartorius Ltd, Epsom,

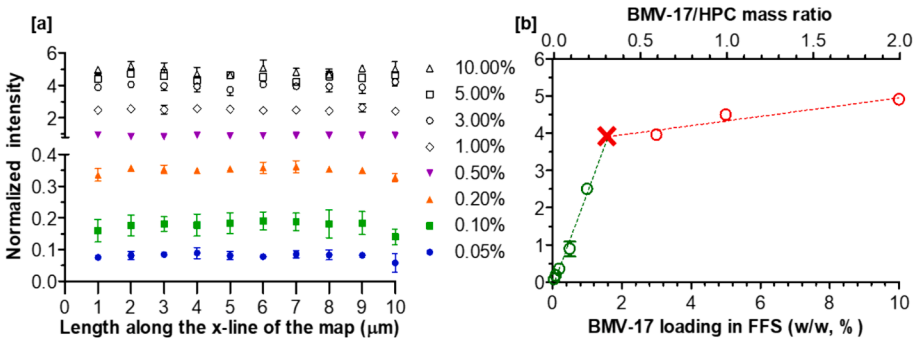

Fig. 4. (a) Normalised, deconvoluted Raman signal intensities from dissolved BMV-17 in the residual films created from FFSs containing between 0.05–10 % drug (mean ± SD of data from three 9 μm lines for each film). (b) Average (±SD) of the normalised drug intensities of the 10 points on each line in panel (a) as a function of both the BMV-17 loading and the drug-to-polymer mass ratio in the residual film (Table 1).

UK). FFSs (1, 3, 5 and 10 % w/w BMV-17) were sprayed or pipetted onto a delimited, 2.01-cm^2 area of a plastic substrate prepared as described previously; the spray delivered 1 g of FFS from a 0.3-mm nozzle, positioned 10 cm from the substrate surface. Post-deposition (i.e., within 1 min or 5 s for sprayed and pipetted films, respectively), the substrate was transferred to the analytical balance where the weight of the evaporating FFS was recorded immediately (time 'zero') and then at 1, 2, 3, 4, 5, 15, 30, 120, 240 min. The experiments were performed in triplicate at 32 °C and 35 % RH. Average values of % mass loss as a function of time (t) were fitted to the Weibull equation (Rinne, 2008)

$$\%\ mass\ loss = \propto\left[1 - \exp\left((t/\tau)^{\beta}\right)\right] \quad (1)$$

where $\propto$ is the maximum mass lost (%), τ is the characteristic time at which the mass loss is 63.2 % (i.e., 100 x (1-e)) of the maximum mass lost, and β is the shape parameter describing the rate of mass loss over time as either decreasing for $t > 0$ ($\beta < 1$), or increasing for $0 < t \leq \tau$ and decreasing thereafter ($\beta > 1$). Best-fit values for $\propto$ and β were determined using OriginPro (2018, Northampton, MA, USA) based on goodness of fit (r^2).

2.11. Data treatment

The percentage of ester group migration was calculated using Eq (2):

$$Drug_{migrated} = \left(\frac{A_{BMV-21}}{A_{BMV-17}}\right)*100 \quad (2)$$

where A_{BMV-21} and A_{BMV-17} denote the amounts of the ester group migration products and acknowledge that, in this study, BM itself was not detected. All IVRT data are reported as the sum of BMV-17 and BMV-21 released into the receptor solution, expressed as the cumulative amount of drug per area (μg/cm^2) or as the flux of drug for each sampling interval (μg/cm^2/h). Flux values were then plotted at the end time of the sampling interval. The applied drug doses (μg/cm^2) were expressed as the total amount of BMV-17. Differences between the mean values of measurements were tested for statistical significance using one-way ANOVA followed by Tukey's test (GraphPad Prism 5, version 9.3.1; San Diego, CA, US). In all the comparisons undertaken, statistical significance was set at $p < 0.05$.

3. Results

3.1. Optimization of spraying parameters

Fast drying films (i.e., those that dried in less than 5 min) were obtained only with the small diameter (0.2 mm and 0.3 mm) spray nozzles, irrespective of the spraying distance (~0, 5, and 10 cm) from the glass surface. Spraying close to the substrate (at ~0 cm or 5 cm) with the small diameter nozzles resulted in films with visually obvious depressions. Homogeneous films were formed when the FFS was sprayed either at 10 cm from the glass surface with the 0.2 or 0.3 mm diameter spray nozzles, or at all distances with the 0.5 mm nozzle. All films were flexible and not sticky. **Table S2** summarizes the observations. Sprayed films in all subsequent studies used the 0.3-mm nozzle at 10 cm from the substrate surface.

3.2. Physical form and distribution of BMV-17 on spray casted films

It was first demonstrated that Raman spectroscopy was able to differentiate between dissolved and crystalline BMV-17 based on the peak frequency of the −C=O vibrational signal (Fig. 2). The presence of drug crystals in residual films after EtOH evaporation from the FFSs containing 1, 3, 5 and 10 % (w/w) BMV-17 was assessed visually and

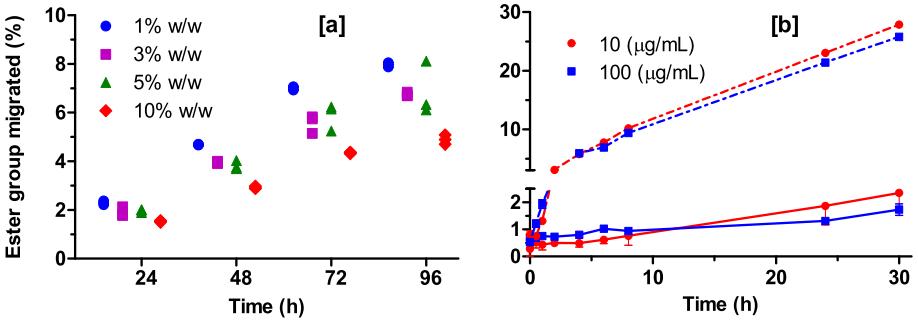

Fig. 5. Ester group migration in (a) FFSs containing 1, 3, 5 and 10 % BMV-17 loadings at 24, 48, 72, and 96 h (three replicates per concentration), and (b) aqueous-based (dashed lines) and organic-based (solid lines) receptor solutions initially containing 10 μg/mL and 100 μg/mL BMV-17 (mean ± SD, n = 3).

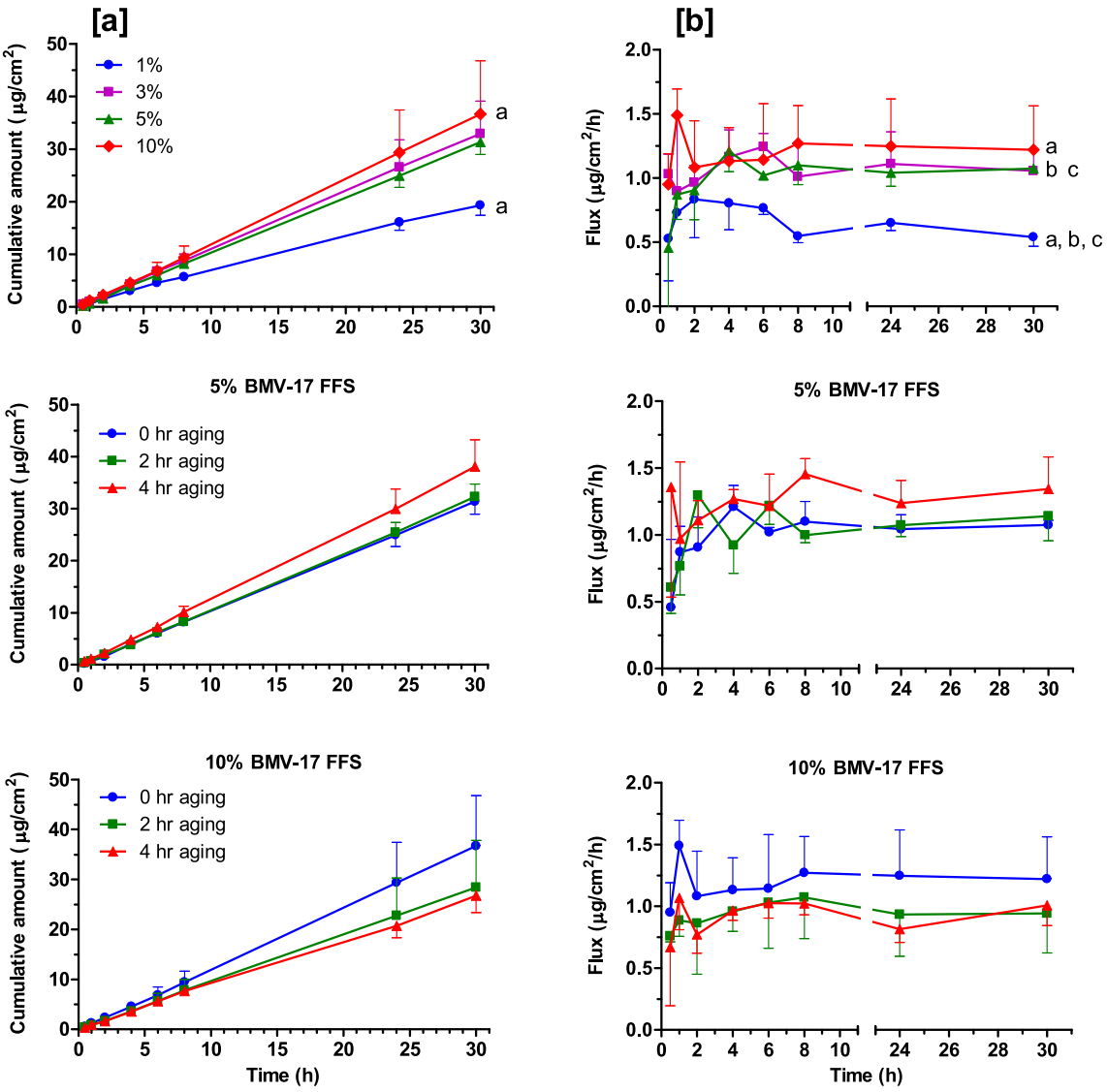

Fig. 6. Cumulative amounts of BMV-17 released (left panels) and drug fluxes (right panels) into the aqueous-based receptor solution as a function of time. Data in the upper panels were acquired from fresh (non-aged) residual films from FFSs containing 1, 3, 5 and 10 % BMV-17 loadings. Results in the middle and lower panels compare fresh and aged residual films from FFS containing 5 % and 10 % BMV-17 loadings, respectively. Drug flux was calculated for each sampling interval and plotted at the end of the interval. Data shown are the mean ± SD (n = 3). Pairs of films at different loading (or aging) that have significantly different cumulative amounts at 30 h or flux over the final 6 h (24–30 h post FFS application) are labelled with the same letter; in the left panels only the fresh films from the 1 % and 10 % loaded FFS were significantly different as indicated by'a' label on each line.

from optical microscopy images of films as shown in **Figure S2** and Fig. 3a, respectively. The residual film formed from the 1 % BMV-17 solution was smooth and transparent with no crystals evident; in contrast, the films from FFSs with higher drug loadings showed individual crystals with a pyramidal habit and other solid aggregates.

Further information on the physical form and distribution of BMV-17 is provided by the corresponding Raman maps of the frequency of the BMV-17 −C=O stretching peak from the four residual films in Fig. 3b. It is noted that these maps do not show the absolute signal intensities or drug concentrations. The colour range in these Raman images varies from almost white through yellow, orange, and red to almost black: the lighter colours are characteristic of dissolved BMV-17 at higher wavenumber (~1666 cm^{-1}), while darker colours reflect crystalline BMV-17 at lower wavenumber (~1659 cm^{-1}); wavenumbers between the two colour extremes result from overlapping peaks originating from a mix of dissolved and crystalline corticosteroid. The map of the residual film from the FFS at 1 % BMV-17 loading, therefore, clearly indicates the presence of only the dissolved form of the drug. In contrast, the maps of the films from FFSs at 3, 5 and 10 % BMV-17 loadings demonstrate the progressively increasing presence of drug crystals.

To distinguish dissolved and crystalline drug further, the Raman signals from BMV-17 were deconvolved and then normalised by the corresponding peak intensity of the HPC polymer (to account for inter-film variability in the spectra). Profiles of the normalised dissolved and crystalline peaks along the dot-dashed lines in Fig. 3b are presented in Fig. 3c, and the corresponding frequencies of the deconvoluted peaks are shown in Fig. 3d. For the residual film from the FFS with 1 % BMV-17 loading, the normalised intensity of the dissolved drug was relatively constant at a value of 2.5; that of the crystalline form was below reliable detection (i.e., within the baseline noise and highly variable).

In the residual films from FFSs containing 3 % or higher drug loadings, the normalised signals from the dissolved BMV-17 at ~1666 cm^{-1} were again relatively constant across the samples with values of about 4–5. This suggests that residual films with BMV-17 levels at 3 % and above are already saturated with the drug. Of course, the images and maps in Fig. 3a and 3b clearly corroborate this deduction by the obvious

Table 2
IVRT experiments with an aqueous-based receptor solution (mean ± SD, n = 3): drug loadings (mass ratio of BMV-17 to FFS non-drug constituents), drug amount applied and released, initial dissolved drug amount in the residual films, and percentage of dissolved and total drug released from the films.

Drug loading in FFS (%)	Aging (h)	Drug applied ($\mu g/cm^2$)	FFS applied (mg/cm^2) [a]	Drug released over 30 h ($\mu g/cm^2$)	Dissolved drug in residual film ($\mu g/cm^2$) [b]	% dissolved drug released in 30 h [c]	% applied drug released in 30 h [d]
1	0	226 ± 74	23 ± 7.5	19 ± 1.9	226 ± 74	9.1 ± 2.7	9.1 ± 2.7
3	0	508 ± 83	17 ± 2.8	33 ± 6.2	271 ± 44	12 ± 3.2	6.6 ± 1.7
5	0	1177 ± 189	25 ± 4.0	31 ± 2.4	377 ± 61	8.4 ± 1.0	2.7 ± 0.3
10	0	1546 ± 157	17 ± 1.7	37 ± 10	247 ± 25	15 ± 5.5	2.4 ± 0.9
5	2	866 ± 222	18 ± 4.7	32 ± 2.4	277 ± 71	12 ± 2.5	3.9 ± 0.8
5	4	896 ± 152	19 ± 3.2	38 ± 5.2	287 ± 49	13 ± 1.4	4.3 ± 0.4
10	2	1323 ± 376	15 ± 4.1	28 ± 9.4	212 ± 60	14 ± 7.0	2.3 ± 1.1
10	4	1351 ± 242	15 ± 2.7	27 ± 3.4	216 ± 39	13 ± 2.9	2.0 ± 0.5

[a] Mass per area of FFS applied to achieve the measured applied drug mass per area (calculated from drug mass fractions in Table 1; see **Table S3).**
[b] Estimated dissolved drug amount after precipitation (calculated as described in **Table S3)** assuming that a FFS containing 1.60 % BMV-17 loading (equivalent to 0.32 w/w drug:polymer) produces a film with the drug at its saturation limit.
[c] Percentage of the drug released over 30 h with respect to the estimated dissolved drug.
[d] Percentage of the drug released over 30 h with respect to the drug applied.

presence of crystalline drug. Fig. 3c further supports the conclusion as the deconvoluted Raman signals from the crystals obviously reflect exactly where the solid form of the drug can be found. In films from the FFSs at the highest drug loadings (5 and 10 %), the values of the normalised signals from the crystalline form of the drug in areas of the map where such structures cannot be perceived are nonetheless well above the baseline noise, again implying that these films are indeed saturated with BMV-17. Of course, when the line profile crosses a visually perceptible crystal, the normalised drug signal (at about 1666 cm^{-1}) is substantially elevated (with values at their highest reaching 10 to >25).

3.3. Estimation of drug equilibrium solubility in the residual film

Raman maps along 9-μm lines were acquired (every 1 μm) from the residual films from FFSs with BMV-17 loadings between 0.05 and 10 %. The deconvoluted peaks of the dissolved drug were then normalised as before using the HPC signals acquired from the same films and the results are shown in Fig. 4a. For films from FFSs with 0.05 to 1 % drug loading, the normalised dissolved drug signal increased linearly with drug loading (slope = 2.5 $\%^{-1}$, $r^2 = 0.98$); in contrast, for films from FFSs with 3 to 10 % drug loading, the corresponding signals were relatively insensitive to the amount of BMV-17 present (slope = 0.13 $\%^{-1}$, r^2 = 0.90) (Fig. 4b). The dramatic change observed in the concentration dependence is evidently due to the drug reaching its equilibrium solubility in the residual film (see previous section), the value of which can be inferred from the intersection of the distinct linear behaviours at low and high BMV-17 loadings in the FFS (or, indeed, as a function of the mass ratio of drug-to-HPC – see Fig. 4b). We deduce, therefore, that 1.60 % is the minimum FFS drug loading that produces a residual film at the saturation limit of 21.1 % BMV-17, which corresponds to a drug-to-HPC ratio of 0.32.

3.4. Profilometry and 3D topography of sprayed films

Profiles of the residual films from FFSs containing 1, 3, 5 and 10 % w/w BMV-17 are presented in Fig. S3a. The thicknesses of the films created from FFSs containing 1 and 3 % BMV-17 were greatest at their edges and then decreased to relatively constant values of 15 – 22 μm and 18 – 32 μm, respectively. Thicknesses of films sprayed from FFSs containing 5 and 10 % w/w BMV-17 were much more variable (10 – 80 μm), presumably due to the significant presence of drug crystals.

The 3D micro-topographies of surfaces of residual films from FFSs containing 1, 3, 5 and 10 % w/w BMV-17 were evaluated directly below (central) and to the side (border) of the spray nozzle using AFM (Fig. S3b). The changes in film height for all drug loadings were in the nanoscale range (<250 nm). Images from the border area of films with ≥3 % BMV-17 exhibited rougher surfaces with craters that were about 100–200 nm below the peaks in these films.

3.5. Ester group migration studies of BMV-17

Ester group migration from BMV-17 to the 21-position was observed in FFSs stored at 32 °C, with about 2 % conversion in the first 24 h and increasing to between 5–8 % after 96 h (Fig. 5a). When films were sprayed after 24-h storage, no further migration than the ~ 2 % seen before occurred over the next 30 h. Ester group migration in the receptor solutions used for drug release studies depended on the composition used. In the aqueous-based receptor solution, ester group migration was ~30 % after 30 h storage at 32 °C and 35 % RH and was independent of drug concentration. In contrast, in EtOH/water 60/40 % v/v, conversion at 30 h was only about 2 % and, again, was insensitive to the initial amount of BMV-17 (Fig. 5b).

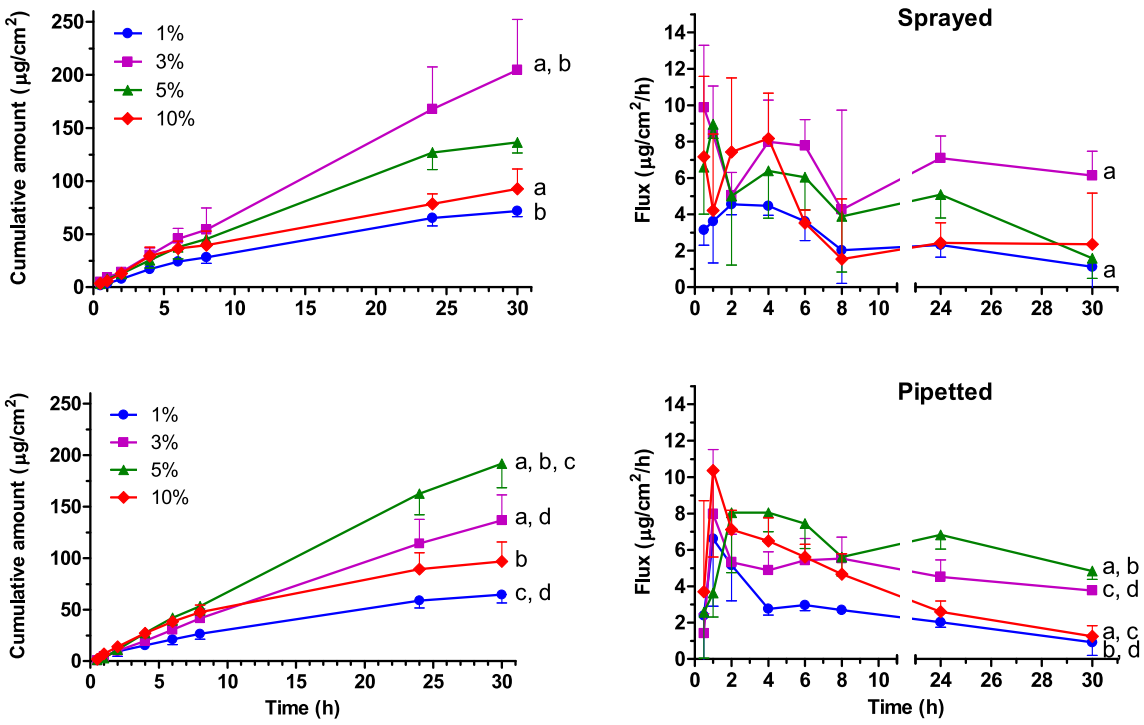

Fig. 7. Cumulative amounts of BMV-17 released (left panels) and drug fluxes (right panels) into the organic-based receptor solution as a function of time. Data in the upper and lower panels were acquired from fresh (non-aged) residual films from sprayed and pipetted FFSs, respectively, containing 1, 3, 5 and 10 % BMV-17 loadings. Drug flux was calculated for each sampling interval and plotted at the end of the interval. Data shown are the mean ± SD (n = 3). Pairs of films at different loading which provided significantly different cumulative amounts at 30 h or flux over the final 6 h (24–30 h post FFS application) are labelled with the same letter; e.g., in the left panel of the sprayed films, the films from the 3 % FFS are significantly different from the 10 % (labeled 'a') and 1 % (labeled 'b') FFS films.

3.6. In vitro release testing (IVRT)

3.6.1. Drug release from sprayed films into an aqueous-based receptor solution

The results from these experiments are presented in Fig. 6 and Table 2. Drug release profiles from fresh (non-aged) films prepared using FFSs with 3, 5 and 10 % BMV-17 loadings were similar and distinct from that from the 1 % drug film (Fig. 6, upper panels), showing the clear demarcation between films in which the drug was saturated (3, 5 and 10 %) and that in which it was not (1 %). For all films, drug release rate increased over the first 30–60 min before reaching relatively constant values; the average fluxes measured in the final 6 h were (mean ± SD, n = 3): 0.54 ± 0.07, 1.06 ± 0.16, 1.07 ± 0.04 and 1.22 ± 0.34 µg $cm^{-2}h^{-1}$ for films containing 1, 3, 5 and 10 % BMV-17 loadings, respectively.

The average flux measured in the final 6 h and the 30-h cumulative drug release from the films were compared by ANOVA followed by Tukey's test. The average flux from the film created by the 1 % FFS was significantly smaller ($p < 0.05$) than those deposited from the 3, 5 and 10 % films; for the cumulative drug released at 30 h, there was a significant difference only between the residual films deposited from the 1 % and 10 % FFSs. No differences (at $p < 0.05$) in either the amounts of drug released over 30 h, or the average flux measured in the final 6 h, were found between the residual films formed from FFSs containing 5 or 10 % BMV-17 loadings that had been aged for 2 or 4 h (Fig. 6, middle and lower panels, and Table 2).

From the estimated drug solubility in the films and the applied amounts of BMV-17, the initial quantities of dissolved drug in the films and the percentage of these quantities released in 30 h were calculated (Table 2). The latter for all films were less than 15 % (including the sub-saturated 1 % film), indicating that the net depletion of BMV-17 in these IVRT experiments was small.

3.6.2. Drug release from sprayed and pipetted films into an organic-based receptor solution

Fig. 7 and Table 3 summarize the data from these IVRT experiments. Controlling the amount of FFS sprayed onto the diffusion area of the silicone membranes proved to be difficult such that the average applied drug doses did not always increase proportionally with BMV-17 content (for example, compare the average applied drug dose in the sprayed residual films from FFSs containing 5 and 10 % BMV-17 loadings). A similar issue occurred with films in the aqueous-based receptor studies above, but to a much lesser extent (Table 2). The experimental design aimed to approximately match the applied drug doses from the sprayed and pipetted films, although this was not always possible; for example, the dose from the FFS with 5 % BMV-17 loading was significantly lower from the pipetted film than that which was sprayed.

Drug release into the organic-based receptor solution clearly differed from that into the aqueous-based one. Most obviously, BMV-17 release into the organic-based receptor solution was significantly greater by factors of 3–6, and much larger fractions of the estimated initial dissolved drug amount (calculated assuming that EtOH in the organic-based receptor solution has not changed the BMV-17 saturation limit in the films) were therefore released; specifically, between 39 and 127 % compared to less than 15 % for experiments with the aqueous-based receptor solution. IVRT with the organic-based receptor solution provided evidence that depletion of the dissolved drug in the film and/or re-dissolution of solid drug occurred. For example, the pipetted film from the FFS containing 5 % BMV-17 loading released more than 100 % of the estimated initial dissolved drug quantity over 30 h. Furthermore, the calculated % released of the initial drug present in the residual films from this set of experiments was always ≥13 %, attaining values of ~40 % in several measurements. It was also the case with the organic-based receptor solution that the cumulative BMV-17 release over 30 h from the sub-saturated residual film (prepared from the FFS containing 1 % drug loading) was less than that from films prepared from the FFS with 3 %

Table 3
IVRT experiments on sprayed and pipetted films with an organic-based receptor solution (mean ± SD, n = 3): drug loadings (mass ratio of BMV-17 to FFS non-drug constituents), drug amount applied and released, initial dissolved drug amount in the residual films, and percentage of dissolved and total drug released from the films.

Drug loading in FFS (%)	Drug applied (μg/cm^2)	FFS applied (mg/cm^2) [a]	Drug released over 30 h (μg/cm^2)	Dissolved drug in residual film (μg/cm^2) [b]	% dissolved drug released in 30 h [c]	% applied drug released in 30 h [d]
Sprayed films						
1	164 ± 27	17 ± 2.8	72 ± 5.5	164 ± 27	44 ± 6.2	44 ± 6.2
3	550 ± 144	19 ± 5.0	205 ± 48	293 ± 77	71 ± 14	38 ± 7.4
5	753 ± 18	16 ± 0.4	136 ± 9.9	241 ± 5.6	57 ± 2.8	18 ± 0.9
10	780 ± 379	8.6 ± 4.2	93 ± 19	125 ± 61	86 ± 38	14 ± 6.0
Pipetted films						
1	166 ± 23	17 ± 2.3	64 ± 7.9	166 ± 23	39 ± 3.9	39 ± 3.9
3	440 ± 105	15 ± 3.6	137 ± 25	235 ± 56	61 ± 21	33 ± 11
5	511 ± 144	11 ± 3.0	192 ± 23	164 ± 46	127 ± 51	41 ± 16
10	740 ± 58	8.1 ± 0.6	97 ± 19	118 ± 9.2	82 ± 18	13 ± 2.9

[a] Mass per area of FFS applied to achieve the measured applied drug mass per area (calculated from drug mass fractions in Table 1; see **Table S3**).
[b] Estimated dissolved drug amount after precipitation (calculated as described in **Table S3**) assuming that a FFS containing 1.60 % BMV-17 loading (equivalent to 0.32 w/w drug:polymer) produces a film with the drug at its saturation limit. EtOH permeation from the organic-based receptor solution through the membrane into the residual film may have increased drug solubility therein.
[c] Percentage of the drug released over 30 h with respect to the estimated dissolved drug.
[d] Percentage of the drug released over 30 h with respect to the drug applied.

(spraying or pipetting) and 5 % (pipetting) loading, in which the drug was saturated. Moreover, unlike the aqueous receptor solution results, some of the saturated films released different amounts of drug at 30 h without obvious trends with FFS loading. In some cases, the release rate appeared to be sustained over the 30-h duration of the study; in others, a noticeable decrease in this metric was observed. The irreproducibility of the 'doses' from the sprayed and pipetted FFSs is probably a key factor in the inconsistency of the data obtained.

3.7. EtOH evaporation

Different EtOH evaporation kinetics during FFS deposition are evident depending on whether spraying or pipetting was used. Notably, while the initial weight of the sprayed films was approximately 8 mg, those pipetted were much higher: 42 ± 2, 33 ± 4, 33 ± 2 and 18 ± 1 mg for the formulations with 1, 3, 5 and 10 % loadings. This difference is primarily the result of the faster evaporation of EtOH during spray deposition and before the first weight measurement was made. In contrast, the FFS mass delivered by pipetting was much more controllable and precise.

Weight loss over time was consistent with ethanol evaporation post-spraying as previously described (Reid et al., 2013) and adequately fitted by the Weibull equation (Eq. (1); Fig. 8) for the best-fit parameter values listed in Table 4. The maximum mass lost, indicated by $\propto$, from the pipetted films is within 2 % of the amounts of EtOH in the FFSs (i.e., 93.1, 91.3, 89.5 and 85.5 % for FFSs containing 1, 3, 5 and 10 % BMV-17 loadings, respectively; **Table S1**). This is consistent with the relatively short time required to pipette the FFS onto the substrate and then make the first measurement. For sprayed films, on the other hand, $\propto$ was smaller by 10–25 % than the % EtOH in the FFS for all films, implying that significant solvent evaporation had occurred before the first measurement of film weight. Of course, this is not surprising given the large surface area-to-volume ratio of the small droplets from the 0.3 mm spray nozzle, which enables significant evaporation before the FFS reaches the substrate, plus the time needed to spray the film, and the ~1 min delay post-spraying before the first weight measurement can be made. The variation in the time at which 63.2 % of the film mass had evaporated (τ) is consistent with the differences in the FFS mass that was pipetted onto the substrate. In contrast, the mass of FFS of all the sprayed films was relatively constant and therefore τ values in this case are quite similar.

The shapes of the evaporation curves at short times (Fig. 8, insets) are different for the sprayed and pipetted films; the behaviours are reflected in the best-fit values for β, which are < 1 for the former (concave up) and > 1 (concave down) for the latter. This is again consistent with significant evaporation from the sprayed films prior to measurement of the % mass loss that was not observed for the pipetted films; that is, the initial mass loss seen for the pipetted films at the shortest times is 'missed' for the sprayed films as it occurred before the weight measurements could begin.

4. Discussion

The aim of this work was to evaluate the impact of dermatological product metamorphosis on drug release from FFSs of relatively simple composition compared to typical topical formulations. Attention was focused on FFSs comprising only four components: specifically, the drug (BMV-17) at different loadings in a volatile solvent (EtOH) with a polymeric film forming agent (HPC) and a plasticizer (TEC). The FFSs were applied principally by spraying – a commonly used application method – to produce films that were homogeneous, fast drying, flexible and non-sticky, i.e., critical attributes for products with superior delivery and cosmetic appeal (Frederiksen et al., 2015).

Residual films after complete EtOH evaporation were characterized by visual examination, optical microscopy, profilometry, AFM and confocal Raman microscopy. Solid structures (consistent with the crystal habit of BMV-17 (Garvie-Cook et al., 2015a)) were observed in the films

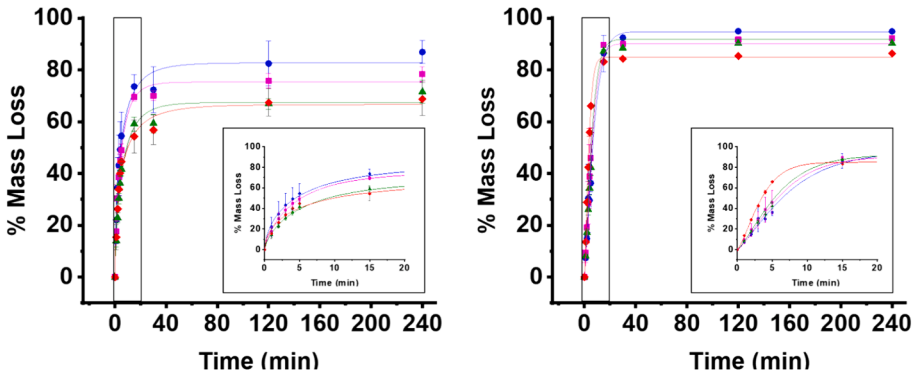

Fig. 8. Mass loss as function of time for the sprayed (left panel) and pipetted (right panel) films (mean ± SD, n = 3) containing 1 % (blue), 3 % (plum), 5 % (green) and10% (red) BMV-17 loadings. Lines correspond to the best-fits of the data to the Weibull equation (Eq. (1). Insets on each panel show expanded views of the mass-loss profiles at short times. (For interpretation of the references to colour in this figure legend, the reader is referred to the web version of this article.)

deposited from FFSs containing 3 % or more loading of the corticosteroid and increased in number with increasing drug loading (Fig. 3, **Figure S2**). No crystalline BMV-17 was present in residual films from FFSs with 1 % BMV-17 loading or less, indicating the drug's solubility therein was between 1 % and 3 % BMV-17 loading in the FFS. Profilometry and AFM showed that residual film thickness was greater around the perimeter but was smaller and more uniform in the central area.

Dissolved and crystalline BMV-17 in the residual films were identified separately using the distinct peak positions of the Raman C=O stretching vibrations at 1666 cm^{-1} and 1659 cm^{-1}, respectively. Raman signals from coexisting dissolved and crystalline BMV-17 were resolved using deconvolution, and the intensities and positions of these deconvoluted C=O stretching vibration peaks correlated with the BMV-17 amount and form (crystalline or dissolved), respectively. Signal intensities were normalised by the HPC intensity (from the same spectra) acting as an internal standard to reduce variability from instrumental factors, and day-to-day and sample-to-sample differences in analytical conditions; the advantages of using this 'normalisation' approach in Raman analyses like those performed here has been demonstrated clearly in the recent literature (Zarmpi et al., 2023).

The deconvoluted Raman signals from dissolved BMV-17 were observed in all residual films. In those formed from FFSs where drug loading was 1 % or less (in which no solid drug was observed), the signal increased proportionally with BMV-17 loading in the original FFSs (Fig. 4); when drug loading was 3 % or more in the FFS and drug crystals were clearly evident, the dissolved signal appeared to almost plateau, consistent with saturation of the BMV-17 in these residual films. The intersection of these two distinct patterns of behaviour (i.e., in the amount of dissolved drug versus FFS loading – see Fig. 4), that is, below 1 % and above 3 % drug loading in the original FFS, was used to provide an estimate of BMV-17′s solubility in the residual film and the corresponding drug-to-polymer ratio at which saturation occurred; these values were 1.60 % drug loading in the original FFS and 0.32, respectively. This new and non-destructive approach to estimate a drug's solubility in a polymer film may be contrasted, for example, with the use of differential scanning calorimetry to determine the phase change of a chemical within a polymer (Edwards et al., 2017).

Deconvoluted Raman signals characteristic of crystalline BMV-17 with intensities above the baseline noise were only detected in the residual films from FFSs containing 3 % BMV-17 loading or more. While these films deposited from FFSs had microscopically visible crystalline drug, the Raman spectra from locations where solid material was not observed still showed non-zero signals at 1659 cm^{-1} suggesting precipitation of BMV-17 in the form of particles smaller than the lateral resolution of the Raman microscope (e.g., nanocrystals).

Ester group migration of BMV-17 to BMV-21 was observed in aqueous media, including the aqueous-based receptor solution (~30 % migration at 32 °C in 30 h); migration was much less than this (<2% in 24 h) in the FFSs and was not observed in the residual films deposited from the FFSs. No ester group migration occurred in the organic-based receptor solution; in addition, no hydrolysis of BMV-21 to betamethasone was detectable in the FFSs, or in either receptor solution, or in any residual film. The only significant impact of these findings, therefore, was that the drug release measured in IVRT experiments using the aqueous receptor were reported as the sum of BMV-17 and BMV-21 to provide a meaningful mass balance with respect to the amount of BMV-17 in the original FFS formulations studied.

In the IVRT experiments with an aqueous-based receptor solution, the maximum concentrations of BMV-17 and BMV-21 measured in the receptor were less than 10 % of the measured aqueous solubility of either ester (188 ± 3 μg/mL); the sink condition was achieved due to the presence of Brij 58® in the receptor solution. Drug release rates after about 6 h were quite constant for FFSs at all BMV-17 loadings. The total drug released over 30 h was relatively insensitive for residual films in which BMV-17 was above its solubility limit (i.e., those deposited from FFSs with ≥3 % drug loading) and greater than that for the films created from the FFS with 1 % BMV-17 loading, in which the drug was completely dissolved. These results are entirely consistent with the changing driving force for diffusion-controlled drug release from residual films containing increasing amounts of BMV-17: drug release increases with increasing concentration up to the point where saturation occurs and at which it effectively plateaus (Shah et al., 1993).

For films with drug concentrations that exceeded the saturation limit, a transient state of supersaturation before crystallisation is expected. The experimental results suggest, however, that supersaturation was short-lived and did not affect drug release in the IVRT experiments with the aqueous receptor solution. For all residual films, including those formed from FFSs with BMV-17 loadings below and above the estimated saturation limit of 1.60 %, the release rate remained quite constant over at least the last 24 h of the experiment, consistent with the fact that significant depletion of the drug from the residual film was relatively modest; Table 2 shows that the maximum percentage of the total drug amount released from the originally deposited film was never more than 9 %, while the maximum percentage of the initially dissolved drug in the film that was released never surpassed 15 %. Therefore, in these experiments, sufficient dissolved drug was present once the films had formed indicating that precipitated drug did not have to redissolve (although it may have) to maintain steady-state drug release until the end of the measurement period.

Drug release into the aqueous-based receptor solution from sprayed films that were "aged" for 2 or 4 h before starting the IVRT experiment produced results that were not distinguishable from those using films that were not aged. This would suggest that EtOH evaporation from the freshly prepared films was essentially complete by the time that the IVRT experiment was underway and that no evidence of a transient period of supersaturation was apparent. The latter conclusion is

Table 4
Drug loadings (mass ratio of BMV-17 to FFS non-drug constituents), initial weight of FFS applied, best-fit values of the Weibull equation (Eq. (1)) parameters, and the estimated EtOH fraction that evaporated before weighing began. Data are mean ± SD, n = 3.

Drug loading in FFS (%)	Initial weight (mg)	α (%)	τ (min)	β	r^2	Estimated EtOH evaporated before weighing began (%)[a]
Sprayed films						
1	7 ± 2	82.7 ± 2.3	5.0 ± 0.6	0.64 ± 0.07	0.99	11.6 ± 8.5
3	10 ± 2	75.3 ± 1.3	4.7 ± 0.3	0.79 ± 0.06	0.99	17.4 ± 3.5
5	8 ± 4	67.5 ± 2.0	6.0 ± 0.8	0.73 ± 0.08	0.99	24.0 ± 4.1
10	10 ± 6	66.6 ± 2.5	5.7 ± 1.0	0.59 ± 0.08	0.98	20.6 ± 9.0
Pipetted films						
1	42 ± 2	94.7 ± 1.9	8.1 ± 0.6	1.25 ± 0.10	0.99	−1.9 ± 0.3
3	33 ± 4	91.8 ± 0.8	6.4 ± 0.2	1.30 ± 0.06	0.99	−0.5 ± 0.3
5	33 ± 2	90.1 ± 0.8	6.8 ± 0.2	1.34 ± 0.06	0.99	−0.7 ± 0.1
10	18 ± 1	84.9 ± 0.6	3.5 ± 0.1	1.37 ± 0.05	0.99	0.7 ± 0.2

[a] Calculated as the difference between % EtOH in the FFS minus ∝ divided by the % EtOH in the FFS; **Table S1** provides % EtOH values in the FFSs.

supported by the EtOH evaporation measurements, which showed that most (~70 %; see Table 4 and the derived Weibull parameters for ∝ and τ) of the EtOH in the FFSs had already evaporated within 6 min post-spraying (including evaporation in the minute before weighing began). In this scenario, therefore, it can be concluded that FFS metamorphosis had no obvious effect on drug release in that it was completed rather rapidly and because the solubility of the drug in the residual film was sufficiently large to then sustain drug release over most of the remainder of the experiment. It is very likely, however, that the composition of the FFS and the drug's solubility – both in the FFS and in the residual film – can be manipulated so that metamorphosis would proceed with different kinetics and produce, as a result, observable differences in the drug release profile (including, under specific circumstances, the potential to elicit supersaturation), as demonstrated previously for the same model compound (Reid et al., 2013).

The IVRT experiments into the 60/40 v/v EtOH/water organic-based receptor solution – in which the solubility of BMV-17 was measured to be 21.4 ± 1.1 mg/mL (i.e., >100-fold that in the aqueous-based receptor solution) – showed quite different behaviour. The cumulative mass of BMV-17 released from the residual films in 30 h was at least 3-fold higher than that into the aqueous-based receptor (Fig. 7, Table 3), corresponding to a significant fraction (39 to 127 %) of the estimated initially dissolved drug in the films. Flux from almost all films (except the 3 % sprayed and 5 % pipetted) decreased after the first few hours in a behavior commonly associated with drug depletion (which is also the likely cause of the flux falling off for the subsaturated residual film deposited from the FFS containing 1 % BMV-17).

The obvious difference between the organic- and aqueous-based receptor solutions is that, unlike water, the EtOH in the former is soluble in the silicone elastomer membrane (Twist and Zatz, 1988). Consequently, EtOH can partition into the membrane from the receptor solution, potentially increasing BMV-17 solubility and/or diffusivity therein. In addition, EtOH can transfer from the receptor solution through the membrane into the residual film, increasing BMV-17 solubility and hence reducing the precipitated drug mass and/or re-dissolving previously precipitated drug. As a result, the actual mass of dissolved drug may be higher than those estimated (Table 3), which were calculated from the Raman measurements on films from which all EtOH had evaporated. Other mechanisms that might have further affected drug release in these IVRT experiments include: (a) evaporative loss of EtOH from the outer surface of the residual film thereby progressively reducing EtOH concentration in the receptor solution over 30 h (this would also reduce the EtOH amounts in the membrane and the residual film), and (b) the uptake of EtOH into the silicone membrane during the 0.5-h equilibration with the receptor solution before FFS deposition facilitating a degree of 'replenishment' of the solvent into the freshly-formed residual films. Because more than one of these mechanisms may have affected drug release, and to different extents depending on the FFS composition, it is difficult to develop a fully unambiguous explanation of the observed results.

Films prepared by pipetted deposition of the FFSs directly onto the silicone membrane provided better control of BMV-17 release, and EtOH evaporation times that were a few minutes longer, than those created by spraying (Fig. 8 and Table 4**)**. These observations are consistent with the somewhat later time of maximum drug flux from the pipetted films (between 1 and 2 h compared with 0.5 to 1 h for those sprayed). Overall, the drug mass released over 30 h was similar for sprayed and pipetted films (Table 3); although some statistically significant differences between films with different initial loadings were apparent, no consistent trends in the data can be deduced. Notably, it was found that the amount of drug released from the residual film deposited from the 5 % pipetted FFS was greater than 100 % of the estimated initial mass of dissolved drug. This may indicate that diffusion of EtOH from the receptor solution into the residual film over time significantly increased the amount of dissolved drug and/or facilitated re-dissolution of previously precipitated drug.

5. Conclusions

Volatile excipients are often present in dermatological formulations to improve drug solubilization. However, post-application of a product to the skin, evaporation and/or percutaneous absorption of such solvents has the potential either to induce a transient state of drug supersaturation and/or eventually precipitation of the active "leaving behind" a residual film with clearly different composition and structure from that originally administered. Loss of the volatile excipients during this 'metamorphosis', therefore, may enhance or impede drug delivery in a time-dependent manner. Moreover, the rate and extent of drug delivery during and after metamorphosis will depend on the physical form of the drug, specifically how much of it is dissolved or solid.

This research aimed to investigate the distribution and physical state of BMV-17 post-transformation of a film-forming formulation and to assess the impact on drug release. Raman spectroscopy, in particular, is demonstrated to be a useful tool with which to characterise the metamorphosis, including drug precipitation, of these simple formulations post-deposition, and to enable, therefore, the assessment and optimisation of drug release, including that from the resulting residual phase. The approach should prove useful in the rational design of improved drug products for topical application to the skin.

For BMV-17 in the simple ethanol, polymer and plasticizer formulation examined here, metamorphosis to the residual film was completed in a few minutes. Drug release from these films increased with drug loading up to the drug saturation limit. Films with drug loadings above saturation contained crystalline drug and released drug at rates that were independent of loading. In all formulations studied, the dissolved drug concentrations in the films were sufficient to sustain drug release across thin silicone elastomer membranes into an aqueous receptor solution for up to 30 h.

CRediT authorship contribution statement

Panagiota Zarmpi: Writing – review & editing, Writing – original draft, Methodology, Investigation, Formal analysis, Conceptualization. **Andrea Pensado:** Writing – review & editing, Methodology, Investigation, Formal analysis, Conceptualization. **Sergey N. Gordeev:** Writing – review & editing, Methodology, Conceptualization. **K.A. Jane White:** Writing – review & editing, Methodology, Funding acquisition, Conceptualization. **Annette L. Bunge:** Writing – review & editing, Methodology, Funding acquisition, Formal analysis, Conceptualization. **Richard H. Guy:** Writing – review & editing, Writing – original draft, Methodology, Funding acquisition, Formal analysis, Conceptualization. **M. Begoña Delgado-Charro:** Writing – review & editing, Project administration, Methodology, Funding acquisition, Formal analysis, Conceptualization.

Declaration of competing interest

The authors declare that they have no known competing financial interests or personal relationships that could have appeared to influence the work reported in this paper.

Data availability

Data will be made available on request.

Acknowledgments

We thank William Hayward and Hristo Gonev (University of Bath) for their expertise in AFM image acquisition. This research was funded by the Leo-Foundation (Project LF16117).

Appendix A. Supplementary data

Supplementary data to this article can be found online at https://doi.org/10.1016/j.ijpharm.2024.124595.

References

Bundgaard, H., Hansen, J., 1981. Studies on the stability of corticosteroids VI. Kinetics of the rearrangement of betamethasone-17-valerate to the 21-valerate ester in aqueous solution. Int. J. Pharm. 7, 197–203. https://doi.org/10.1016/0378-5173(81)90105-8.

Bunge, A.L., 1998. Release rates from topical formulations containing drugs in suspension. J. Control. Release 52, 141–148. https://doi.org/10.1016/s0168-3659(97)00211-3.

Chang, R.K., Raw, A., Lionberger, R., Yu, L., 2013. Generic development of topical dermatologic products: formulation development, process development, and testing of topical dermatologic products. AAPS J. 15, 41–52. https://doi.org/10.1208/s12248-012-9411-0.

Davis, A.F., Hadgraft, J., 1991. Effect of supersaturation on membrane transport: 1. Hydrocortisone acetate. Int. J. Pharm. 76, 1–8. https://doi.org/10.1016/0378-5173(91)90337-N.

Edwards, A., Qi, S., Liu, F., Brown, M.B., McAuley, W.J., 2017. Rationalising polymer selection for supersaturated film forming systems produced by an aerosol spray for the transdermal delivery of methylphenidate. Eur. J. Pharm. Biopharm. 114, 164–174. https://doi.org/10.1016/j.ejpb.2017.01.013.

FDA, 2022. Physicochemical and structural (Q3) characterization of topical drug products submitted in ANDAs, Draft Guidance, https://www.fda.gov/regulatory-information/search-fda-guidance-documents/physicochemical-and-structural-q3-characterization-topical-drug-products-submitted-andas.

Frederiksen, K., Guy, R.H., Petersson, K., 2015. Formulation considerations in the design of topical, polymeric film-forming systems for sustained drug delivery to the skin. Eur. J. Pharm. Biopharm. 91, 9–15. https://doi.org/10.1016/j.ejpb.2015.01.002.

Frederiksen, K., Guy, R.H., Petersson, K., 2016. The potential of polymeric film-forming systems as sustained delivery platforms for topical drugs. Expert Opin. Drug Deliv. 13, 349–360. https://doi.org/10.1517/17425247.2016.1124412.

Garvie-Cook, H., Frederiksen, K., Petersson, K., Guy, R.H., Gordeev, S., 2015a. Characterization of topical film-forming systems using atomic force microscopy and Raman microspectroscopy. Mol. Pharm. 12, 751–757. https://doi.org/10.1021/mp500582j.

Garvie-Cook, H., Frederiksen, K., Petersson, K., Guy, R.H., Gordeev, S.N., 2015b. Biophysical elucidation of the mechanism of enhanced drug release and topical delivery from polymeric film-forming systems. J. Control. Release 212, 103–112. https://doi.org/10.1016/j.jconrel.2015.06.015.

Leichtnam, M.L., Rolland, H., Wüthrich, P., Guy, R.H., 2006a. Enhancement of transdermal testosterone delivery by supersaturation. J. Pharm. Sci. 95, 2373–2379. https://doi.org/10.1002/jps.20669.

Leichtnam, M.L., Rolland, H., Wüthrich, P., Guy, R.H., 2006b. Formulation and evaluation of a testosterone transdermal spray. J. Pharm. Sci. 95, 1693–1702. https://doi.org/10.1002/jps.20641.

Lippold, B.C., Schneemann, H., 1984. The influence of vehicles on the local bioavailability of betamethasone-17-benzoate from solution- and suspension-type ointments. Int. J. Pharm. 22, 31–43. https://doi.org/10.1016/0378-5173(84)90043-7.

Moser, K., Kriwet, K., Froehlich, C., Kalia, Y.N., Guy, R.H., 2001. Supersaturation: Enhancement of Skin Penetration and Permeation of a Lipophilic Drug. Pharm. Res. 18, 1006–1011. https://doi.org/10.1023/A:1010948630296.

Oakley, R., Arents, B.W.M., Lawton, S., Danby, S., Surber, C., 2021. Topical corticosteroid vehicle composition and implications for clinical practice. Clin. Exp. Dermatol. 46, 259–269. https://doi.org/10.1111/ced.14473.

Parks, J.M., Cleek, R.L., Bunge, A.L., 1997. Chemical release from topical formulations across synthetic membranes: infinite dose. J. Pharm. Sci. 86, 187–192. https://doi.org/10.1021/js9603010.

Reid, M.L., Benaouda, F., Khengar, R., Jones, S.A., Brown, M.B., 2013. Topical corticosteroid delivery into human skin using hydrofluoroalkane metered dose aerosol sprays. Int. J. Pharm. 452, 157–165. https://doi.org/10.1016/j.ijpharm.2013.04.083.

Rinne, H., 2008. The Weibull Distribution: A Handbook, 1st ed. Chapman and Hall/CRC.

Shah, V.P., Behl, C.R., Flynn, G.L., Higuchi, W.I., Schaefer, H., 1993. Principles and criteria in the development and optimization of topical therapeutic products. Skin Pharmacol. 6, 72–80. https://doi.org/10.1159/000211090.

Surber, C., Knie, U., 2018. In: Surber, C., Abels, C., Maibach, H. (Eds.), pH of the Skin: Issues and Challenges, Curr. Probl. Dermatol, 54. S Karger AG, Basel, pp. 152–165. https://doi.org/10.1159/000489529.

Surber, C., Davis, A.F., 2002. Bioavailability and bioequivalence of dermatological formulations. In: Walters, K.A. (Ed.), Dermatological and Transdermal Formulations, 1st ed. CRC Press, pp. 401–498. https://doi.org/10.1201/9780824743239.

Twist, J.N., Zatz, J.L., 1988. Membrane-solvent-solute interaction in a model permeation system. J. Pharm. Sci. 77, 536–540. https://doi.org/10.1002/jps.2600770616.

Zarmpi, P., Tabosa, M.A.M., Vitry, P., Bunge, A.L., Belsey, N.A., Tsikritsis, D., Woodman, T.J., Delgado-Charro, M.B., Guy, R.H., 2023. Confocal Raman Spectroscopic Characterization of Dermatopharmacokinetics Ex Vivo. Mol. Pharm. 20, 5910–5920. https://doi.org/10.1021/acs.molpharmaceut.3c00755.